Journal of Power Sources 237 (2013) 215–228

Contents lists available at SciVerse ScienceDirect

Journal of Power Sources

journal homepage: www.elsevier.com/locate/jpowsour

Accurate battery pack modeling for automotive applications

Jianwei Li, Michael S. Mazzola*

Center for Advanced Vehicular Systems, Mississippi State University, 200 Research Blvd., Starkville, MS 39759, United States

HIGHLIGHTS

- Modeling at the battery pack level (vs. cell level) for automotive applications.
- Using one simple model rather than aggregating hundreds for pack representation.
- Building model based on the bandwidth of the stimulus by assigning time constants.
- Model robustness is proved on four Ultralife 14.4 V, 6.8 Ah lithium-ion battery modules.
- High fidelity is proved on an A123 360 V, 21.3 kWh lithium-ion battery pack.

ARTICLE INFO

Article history:
Received 19 August 2012
Received in revised form
12 February 2013
Accepted 1 March 2013
Available online 14 March 2013

Keywords:
Batteries
Modeling
Automotive
Lithium-ion
State of charge
Bandwidth

ABSTRACT

This paper describes an advanced battery pack modeling method for automotive applications. In contrast to the common approach of aggregating hundreds of battery cell models in series and parallel for battery pack representation, a simple yet accurate electrical analogue battery model with constant parameters is used to represent the whole battery pack. The modeling process involves only the external characteristics of the battery pack, thus detailed knowledge of the physical construction of the battery pack or the physical parameters of the battery cells are avoided. Battery experimental tests include an independent pulse charging/discharging cycle test and several performance estimates acquired from the anticipated battery application. This modeling approach is achieved by anticipating the bandwidth of the battery application and then optimizing the bandwidth of the battery pack model with this knowledge. The reported work enables a fast dynamic battery pack simulation with a new level of high fidelity. Although the scope of this work does not include temperature and lifetime effects, it is shown that the form of the model and the parameter extraction procedure can encompass these important improvements. This approach was experimentally verified on a 360 V, 21.3 kWh lithium-ion battery pack operated in a plug-in hybrid electric vehicle.

1. Background

An accurate battery pack model is of significant importance for electric drive vehicle drivetrain design and simulation. It is not uncommon to see simple resistance battery models used in vehicle simulations or energy storage system simulations [1,2] even involving fast dynamics in vehicle power delivery. In contrast to the view that vehicle system level simulation does not require highly accurate battery models [3], a high fidelity battery pack model is critical for the vehicle simulation because the drivetrain power management, the motor/generator control, AC/DC & DC/DC converter design and control, the battery pack state of power (SOP) management, etc. are highly dependent on the accurate prediction of the battery power and battery state of charge (SOC). This is true largely because of the fast dynamics of the battery current when the battery pack is used in a real-world electric drive vehicle, e.g., electric vehicle (EV), hybrid electric vehicle (HEV), and plug-in hybrid electric vehicle (PHEV). As a result, simple models with existing modeling methods are not capable of predicting the dynamic responses of the battery pack, which can limit the validity of the entire simulation.

Battery packs usually consist of hundreds of battery cells connected in series and parallel, including battery packs made up of several battery modules, with each battery module containing multiple battery cells in series, parallel, or series–parallel configuration. Much battery modeling work has been reported at the battery cell level [4–9], with little work reported in the literature discussing battery models at the battery pack level, leaving the work of integrating cell models into pack models to the system level designer or power electronics designer who do not have

* Corresponding author. Tel.: +1 662 3255435; fax: +1 662 3255433.
E-mail addresses: lijwing@gmail.com, jl668@msstate.edu (J. Li), mazzola@ece.msstate.edu (M.S. Mazzola).

0378-7753/$ – see front matter © 2013 Elsevier B.V. All rights reserved.
http://dx.doi.org/10.1016/j.jpowsour.2013.03.009

expertise in batteries. Going from battery cell model to battery pack model is not simply aggregating cell models to make a pack model, because in this way not only will it introduce unnecessary computational requirements for system simulation, but also because some phenomena that can only be observed in the battery pack are ignored [10]. Significant fidelity loss will occur if inadequate attention is paid to the battery pack behavior, as opposed to cell-level modeling. Thus it is worth investigating the construction of a battery pack model separately from the cell model.

2. Introduction

Three approaches for battery pack modeling are available in the literature. The first approach is aggregating cell models in series and parallel to represent the battery pack model [11,12]. This approach requires the least effort going from the cell model to pack model, as the only information needed is the cell configuration in the battery pack. However, serious loss of fidelity can occur in the resulting battery pack model as a result of ignoring the cell variations, thermal unbalancing in the battery pack, etc. At the same time, in reality not all battery cells used in battery packs are even available to the actual system designers for battery cell modeling.

The second approach is to scale the cell model into a battery pack model with one simplified model representing the battery pack [13,14]. In this case, the cell discrepancy issues related only to the battery pack are investigated and included in the pack model. Compared with the first approach, the second approach is comprehensive and fast in simulation, which is more suitable for system level design and simulation. Nonetheless, the investigation of cell discrepancy and thermal distribution in a battery pack requires extensive time and effort, and sometimes the battery cells are not readily available to the system designers.

The third approach is building a battery pack model directly on a well-built battery pack with a single battery model capturing the totality of the pack behavior [15–17]. In this case, the characteristics of the battery cells and thermal influences on them are naturally included into the battery pack model, as a result of cumulative effects of cell averaging, and at the same time the battery model will be fast in simulation requiring comparatively little computational power. Another advantage of this procedure is that non-idealities known to exist in battery packs, such as weak cells and interconnection impedances, is captured self-consistently at the time the battery pack model is built. This approach requires no cell-level details or pack configurations, and some modeling algorithms at this level are even independent of battery chemistry. For commercially available battery packs, this approach may be the only possible approach, as in this case battery tests need only be conducted at the battery pack level. Prerequisites for this approach include 1) the battery cells are reasonably well balanced with means for regular cell balancing, and 2) the battery pack should be effectively cooled/heated so that the battery pack does not encounter uncontrolled temperature variations. In other words, only when a well-designed battery system is available can one confidently model the battery pack as a single battery model. The issue of battery cells variation has been discussed in many papers and communications [13,18], and a two-step screening process has been proposed in Ref. [13] to ensure a stable configuration of a battery pack. And many cell equalization approaches have been proposed [1] as well.

Comparing the three battery pack modeling approaches discussed above, the third approach which builds a battery pack model directly on battery pack terminal measurements seems to be the most promising for system level designer. However, large modeling errors up to 3.1% for this battery pack modeling approach even with moderate real-world test regimes were reported in the literature [15–17], which needs to be improved for stringent high fidelity system level simulations. An advanced direct battery pack modeling approach is the subject of this paper.

The focus of this paper is introducing an accurate battery pack modeling approach using an electrical analogue battery model. A high level of model accuracy (less than 1.11% error) for a 360 V, 21.3 kWh lithium-ion battery pack is achieved by correlating the bandwidth of the battery model with the bandwidth of the battery application [19]. Since a real-world battery is a continuous nonlinear system which involves complex reactions between anode and cathode, if exponential terms are used to approximate the battery behavior, no natural exponential moments should be expected because of the nonlinearity of the underlying processes. The electrical analogue battery model, which has been the subject of many modeling papers addressing different formats and different chemistries, is actually a truncated multi-term exponential approximation. Thus there are no natural time constants in these models arising from a physical or chemical analysis. Instead, we argue that the limited number of time constants available in the battery model should be based on the users' simulation objectives [20]. This relationship between achievable model bandwidth and application need is ignored in most scenarios. Instead, much work has been done seeking natural moments for the exponential terms [15,16,21], where the model parameters including the time constants that define the bandwidth of the battery model are estimated to give the "best fit" of an arbitrary load stimulus during the battery test. Large modeling errors are reported in these papers compared to that reported in this paper. The alternative advocated here is to base the bandwidth of the model on the bandwidth of the battery application; and when this is done significantly higher fidelity can be achieved for an electrical analogue battery model of the same order of dynamic approximation. In short, the bandwidth of the battery pack model is chosen as the bandwidth of the actual battery pack application in this work [20].

The work reported here starts by modeling a 14.4 V, 6.8 Ah lithium-ion battery module with detailed parameter estimation, then the robustness of the modeling approach is investigated by applying the extracted module model on four different battery modules of the same type using a different test profile than that used to extract the parameters (albeit with similar bandwidth). Finally, a model of a 360 V, 21.3 kWh lithium-ion battery pack using the same approach is extracted and verified. Results show less than 1.11% modeling error of the lithium-ion battery pack in a drive cycle test when installed on a PHEV.

This paper is organized as follows. Section 1 presents the background of battery pack modeling. Section 2 discusses different pack level battery modeling approaches and the one selected in this work. Section 3 introduces the electrical analogue battery model and its limited bandwidth characteristics. Section 4 describes the parameter estimation algorithm in detail. Section 5 shows the experimental results on an Ultralife UBBL10 lithium-ion battery, with the completed model verified on four battery modules of the same kind. Section 6 shows the experimental results on an A123 360 V, 21.3 kWh lithium-ion battery pack in real-world application. The completed model was verified with vehicle drive cycle test. Section 7 concludes this paper.

3. The battery model

3.1. A review of battery models

There are two general types of battery models available in the literature: the electrochemical battery model and the behavioral battery model, of which the latter comes in both mathematical

formulations and electrical circuit formulations [4,5,12]. The electrochemical battery models [22,23] are comprehensive and intended for battery structure and material design, which usually require intense computation and thus are not suitable for system level simulation. Models of the mathematical form generally consist of formulas derived from curve fitting and are fast in simulation, but they are less accurate compared with other types of battery models [24]. The electrical circuit formulations based on electrical analogue battery models [4,5,7,8] use ideal electric circuit elements such as voltage sources, current sources, resistors, capacitors and inductors to model battery behavior. The complexity and accuracy of the electrical analogue battery models lie between the electrochemical models and the mathematical formulations [4,12]. Since the electrical models are based on electric circuit elements, they are inherently suitable for solution by simulation software with the capability for circuit analysis, such as MATLAB/Simulink and SPICE, and can be easily implemented into larger simulation environments for system level design and simulation.

Various electrical analogue battery models that could give accurate voltage and SOC estimations have been reported in the literature [4,5,12]. Nonetheless, there is little work detailing the bandwidth dependency of the electrical analogue battery model, which is critical to properly understanding and using this model. Due to the way the parameters of most models are estimated, the model itself is a convolution of both the battery characteristics and the user defined model bandwidth. In other words, the parameters of the electrical analogue battery model are directly tied to the design of the dynamic response of the model. An understanding of this principal is critical to properly derive a behavioral approximation for a real-world battery.

3.2. On-line vs. off-line

Battery models can be used in two ways: on-line (i.e., "realtime", primarily for battery SOC estimation, and off-line, mainly aimed at system level design or simulation, e.g., assisting the development or design of a PHEV. Unlike filter based (e.g., Kalman filter) parameter estimation approaches [25–27] which usually work as part of on-line SOC estimation systems, the proposed approach is aimed at battery modeling for off-line system level design and simulation, where accuracy in open-loop simulation is very important.

3.3. The electrical analogue battery model

The electrical analogue battery model [4] is an electric circuit representation of a real-world battery designed to functionally predict battery performance (Fig. 1). Although this model was originally developed for and tested on small format batteries in Refs. [4], this model has proven to be robust when applied to larger format batteries as detailed in this work. Furthermore, it is also shown to be capable of accurately modeling multiple chemistries such as lithium-ion, Nickel-Metal-Hydride (NiMH), and lead-acid batteries [4]. The term "electrical analogue battery model" is introduced to emphasize the fact that although electric circuit components are used in the battery model, they do not represent the internal electrical components of a real-world battery, but instead form an electrical analogue of a state-variable representation of the behavior of the battery as observed at the battery terminals. An electrical analogue model is convenient to use in the typical electrical simulation environment.

This model contains two parts: a state of charge calculator (left) and the electric circuit representation (right). The state of charge is calculated from coulomb-counting with measured terminal current as its input:

$$\mathrm{SOC} = \mathrm{SOC}(0) + \frac{\int_0^t i(t)\mathrm{d}t}{C} \tag{1}$$

where C is battery capacity in A*sec, and $i(t)$ is battery terminal current in A.

The electric circuit representation consists of a controlled voltage source, a series resistor and N sets of RC networks. This portion of the model comprises the electrical part that represents the battery dynamic characteristics. The series resistor is responsible for the instantaneous voltage drop [4,7] during charging/discharging as tied to the time based resolution of the data, and the RC networks approximate non-linear transient responses with the equivalent of a truncated exponential series. The number of RC networks determines the resolution of the model dynamic responses. These two parts are connected by a State of Charge–Open Circuit Voltage (OCV) mapping, which is represented by a polynomial equation. In Eq. (1), the positive direction for current has been taken to be when the battery is charging (negative sign for discharging). Although electrical components are used in the electrical analogue battery model, they do not represent the internal electrical construction of a real-world battery, but rather form a behavioral approximation of the terminal characteristics.

3.4. The limited bandwidth of the electrical analogue battery model

A real-world battery is a continuous non-linear system [4,6,9], involving complex electrochemical reactions between anode and cathode. Since a finite number of RC networks are used in the circuit part of the battery model, the RC networks are actually a truncated series exponential representation of a non-linear real-world battery system. There are no natural exponential moments associated with the real-world battery as a result of the non-linearity. Thus the exponential moments should be chosen to give the best approximation of the battery responses based on the user defined load stimulus. When loads with different spectrums are used for curve fit based parameter estimation with exponential basis functions there

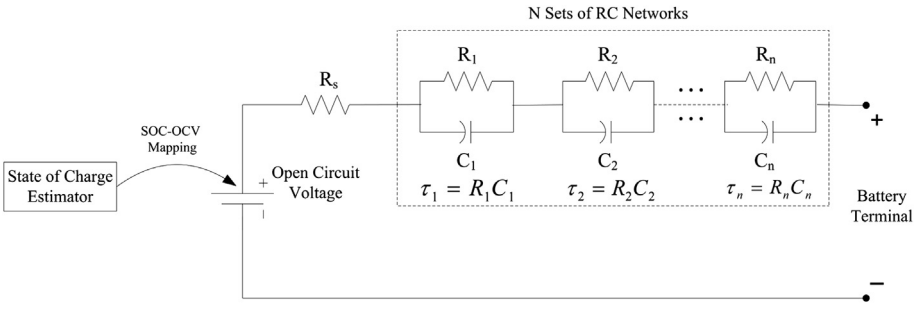

Fig. 1. The electrical analogue battery model [19].

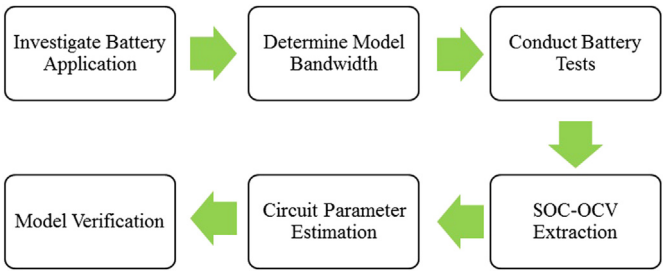

Fig. 2. The work flow of the modeling procedure.

exists a dependency of the resulting moments on the load stimulus. This dependency is usually ignored in the literature, in which case the battery model is considered applicable to any load once the model is built even though it is based on a certain load stimulus. However, significant fidelity loss will result if the battery is used in an environment where the load is significantly different from the load stimulus used to build the battery model.

Alternately, this phenomenon can be explained from the bandwidth aspect of the model. The bandwidth of the battery model is determined by the time constants of the RC networks in the electric circuit representation. When a finite number of RC networks approximate the dynamic response of the battery, the model is discrete in simulation with limited bandwidth. It is common to identify the bandwidth of a physical system for modeling and control purposes; nonetheless, the limited bandwidth characteristic of the electrical analogue battery model – a finite approximation of a real-world battery with potentially much wider bandwidth – is ignored in most scenarios.

Take the first RC network in the battery model as an example. The natural response of the RC network is:

$$V_1(t) = V_1(0)\exp\left(-\frac{t}{\tau_1}\right) \tag{2}$$

where τ_1 is the time constant of the RC network.

The voltage $V_1(t)$ on the RC network will decrease to 5% of the initial value in $3\tau_1$. Transient responses longer than several times of τ_1 will not be adequately approximated by this RC network. In general, the bandwidth of the electrical analogue battery model is limited to $[1/\tau_{max}, 1/\tau_{min}]$, where $\tau_{min}$is the smallest time constant among the included RC networks and τ_{max} is the largest time constant among the included RC networks.

Realizing the bandwidth limitation characteristic of the electrical analogue battery model, the time constants of the RC networks should be selected based on the desired frequency range of the battery application, rather than an arbitrary battery experimental test. As a consequence, the load stimulus of the battery experimental test should be designed to accommodate the battery application frequency range for high fidelity battery modeling.

Another frequency related factor of the model is the sampling frequency of the battery experimental test. The sampling frequency should be chosen based on the frequency of the battery application and the model fidelity requirements. For example, if the sampling frequency of the experimental battery test is 1 Hz, then battery dynamics faster than 0.5 Hz will not be accurately modeled. In other words, a battery model built on a particular sampling frequency is not supposed to be used in a simulation with shorter computational time steps because of the possibility of aliasing.

4. Model parameter extraction

4.1. Overview

The proposed work flow of the modeling procedure is summarized as Fig. 2. The parameter estimation algorithm should be designed to accommodate the limited bandwidth characteristic of the electrical analogue battery model. It is necessary to investigate the battery application prior to constructing the model. The bandwidth of the battery application will determine the bandwidth of the battery model, which in turn determines the time constants of the RC networks. Two battery tests, which we call “behavioral” tests, should be conducted for the modeling purpose, one is for the

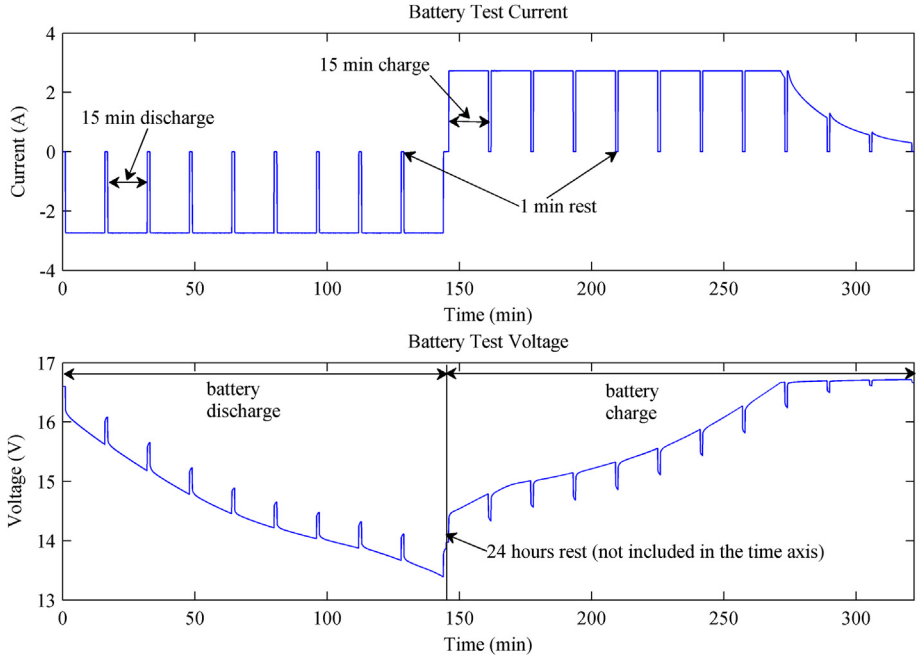

Fig. 3. The battery pulse charging/discharging cycle for the SOC–OCV profile extraction [19].

SOC–OCV profile extraction, and the other is for the circuit parameter estimation. After the battery tests, the SOC–OCV profile and circuit parameters can be estimated with the proposed algorithm. The last step is model verification, where the completed battery model will be tested with different loads, a process we call "performance" testing.

4.2. Model bandwidth and the number of RC networks

If the bandwidth of battery application is $[f_{low}, f_{high}]$, then the smallest and the largest time constants of the RC networks in the battery model should be selected as $\tau_{min} = 1/f_{high}$ and $\tau_{max} = 1/f_{low}$. The number of RC networks with time constants between $[\tau_{min}, \tau_{max}]$ should be determined based on the fidelity requirement of the model. If a simple model with the least computational burden is desired, the number of RC networks can be two. If fidelity of the model is the first concern, the number of RC networks can be 3, 4...N.

4.3. SOC–OCV profile extraction

A battery pulse charging/discharging cycle is required for the SOC–OCV profile extraction. As illustrated in Fig. 3, the battery was pulse discharged from full SOC to about 10% SOC and then pulse charged back to full to extract the SOC–OCV profile [9]. The charging pattern was determined based on the battery datasheet. Particularly, for the charging test illustrated in Fig. 3, the turn from constant current charging to constant voltage charging happened when the battery terminal voltage reached 16.6 V, as defined in the battery datasheet [28]. The SOC test range of [10%, 100%] is selected to embrace the normal battery operating ranges without the risk of causing irreversible changes to battery physical structures by overly deep discharging. The pulse length is chosen to discharge or charge the battery by 10% SOC, while allowing the battery to rest for 1 min between each pulse to observe the battery dynamics during relaxation. The battery was allowed to rest for 24 h between discharging and charging.

In Fig. 4, battery terminal voltage during the test is plotted versus SOC. The extracted SOC–OCV profile is shown as the red line in Fig. 4. This line is achieved by averaging the dotted green line and the dotted blue line, which are the voltage settling points in the rest periods during battery charging and battery discharging, respectively [9]. Further, for a more accurate SOC–OCV profile, the battery can be pulse discharged and charged with a 24 h rest period between two succeeding pulses within the desired SOC operating

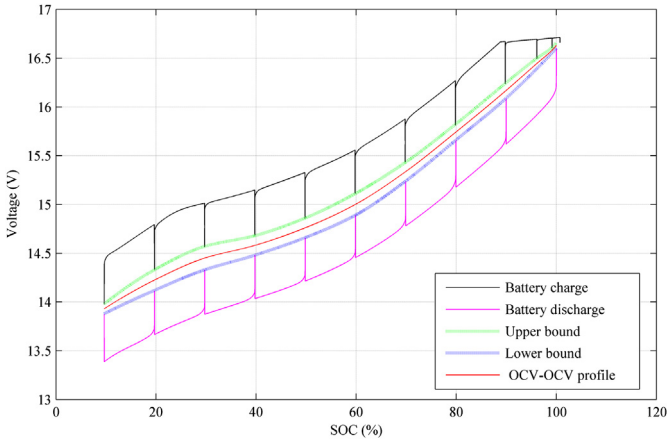

Fig. 4. Battery SOC–OCV profile extraction [19].

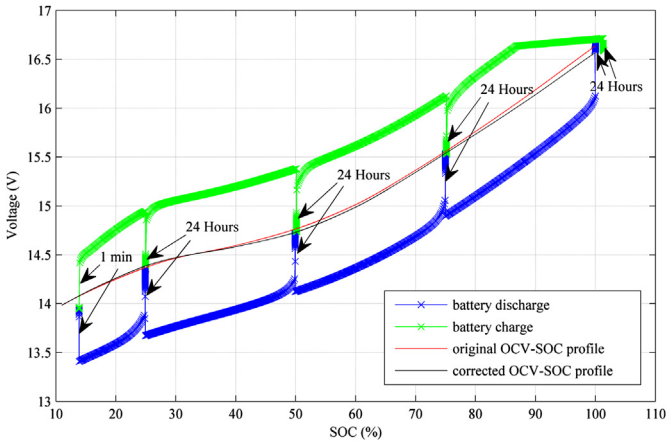

Fig. 5. Correction of the extracted SOC–OCV profile [19].

range to allow the battery voltage to reach its true OCV (Fig. 5), in which way the initially extracted SOC–OCV profile was corrected for additional accuracy in the desired SOC operating range by taking advantage of the improved estimate of the open-circuit voltage observable at the battery terminal after 24 h [9].

4.4. Circuit parameter estimation

4.4.1. Behavior battery test

To estimate the circuit component parameters, a behavior battery test with frequencies close to $[f_{low}, f_{high}]$ should be conducted for parameter estimation. Sampling the terminal variables of a battery while it is used in an application is an attractive alternative for batteries in commercial use. The choice of load stimulus is arbitrary as long as it has sufficient frequency components that correlate with the anticipated bandwidth of the simulation using the resulting model. The term "behavior test" was defined here as when the measured battery terminal current and terminal voltage are known to the battery model for the purpose of parameter estimation. Later, the term "performance test" will be introduced when only the measured terminal current is known to the battery model but the measured terminal voltage is unknown to judge the model accuracy by comparing the measured terminal voltage and the model output.

4.4.2. Mathematical description of the model

A two-RC network representation of the battery model is the level of approximation commonly found in similar advanced work and was thus also selected for this work as illustrated in Fig. 6. The mathematical equations for the two-RC network are derived as Eqs. (3) and (4):

$$\begin{bmatrix} \dot{V}_{c1} \\ \dot{V}_{c2} \\ \dot{\mathrm{SOC}} \end{bmatrix} = \begin{bmatrix} -\frac{1}{R_1C_1} & 0 & 0 \\ 0 & -\frac{1}{R_2C_2} & 0 \\ 0 & 0 & 0 \end{bmatrix} \begin{bmatrix} V_{c1} \\ V_{c2} \\ \mathrm{SOC} \end{bmatrix} + \begin{bmatrix} \frac{1}{C_1} \\ \frac{1}{C_2} \\ \frac{1}{C} \end{bmatrix} i_t \tag{3}$$

$$V_t = V_{ocv}(\mathrm{SOC}) + R_s i_t + V_{c1} + V_{c2} \tag{4}$$

where V_{c1}, V_{c2}, SOC are capacitor C_1, C_2 voltages and battery SOC, respectively. The parameters which need to be estimated are R_s, R_1, C_1, R_2, and C_2. Battery capacity C in Eq. (3) is assumed to be a constant. Battery open circuit voltage $V_{ocv}(\mathrm{SOC})$ is an eighth-order polynomial equation in SOC representing the SOC–OCV mapping.

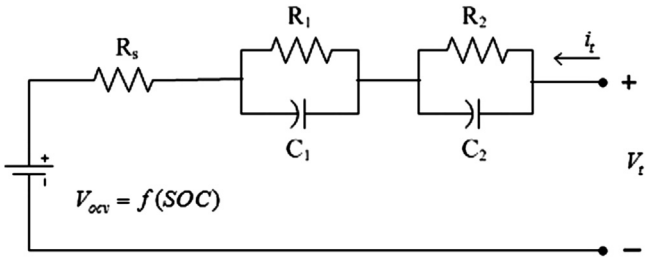

Fig. 6. The two-RC network representation of the battery model.

4.4.3. Sequential Quadratic Programming

Sequential Quadratic Programming (SQP) is used for parameter estimation. The objective function is formed as the error between the measured battery terminal voltage from the behavior test and the model terminal voltage output with the behavior battery test current as load stimulus. And then SQP is used to minimize the objective function by varying the circuit parameters R_s, R_1, C_1, R_2, and C_2.

Define:

$$Z = [R_s\ R_1\ C_1\ R_2\ C_2]^T \tag{5}$$

The minimization problem is summarized as:

Minimize:

$$f(Z) = \sum_{i=1}^{n}\left(V^i_{t-\mathrm{mea}} - V^i_{t-\mathrm{sim}}\right)^2 \tag{6}$$

Subject to:

$$\begin{aligned} h_1(Z) &= R_1C_1 - \tau_1 = 0 \\ h_2(Z) &= R_2C_2 - \tau_2 = 0 \\ R_s,\ R_1,\ C_1,\ R_2,\ C_2 &> 0 \end{aligned} \tag{7}$$

where $V^i_{t-\mathrm{mea}}$, $V^i_{t-\mathrm{sim}}$ are the measured battery terminal voltage and model output voltage, respectively.

The Lagrange function is formed as

$$L(Z) = f(Z) + \sum_{m=1}^{2}\lambda_m h_m(Z) \tag{8}$$

where λ_m is the Lagrange multiplier associated with equality constant h_m.

Let $d^k = \Delta Z^k$ be a five-dimensional search direction vector, the quadratic programming sub-problem at a specific design point is formulated [29,30] as,

Minimize:

$$Q\left(d^k, Z^k\right) = \nabla f\left(Z^k\right)^T d^k + 0.5\left(d^k\right)^T B^k d^k \tag{9}$$

Subject to:

$$h_m\left(Z^k\right) + \nabla h_m\left(Z^k\right)^T d^k = 0 \quad m = 1,2 \tag{10}$$

where B^k is a positive definite matrix used to approximate the Hessian of the Lagrange function $L(Z)$.

This is a typical SQP problem that could be solved using the standard SQP algorithm [29,30]. The optimum solution to this SQP problem is the optimum Z, which represents the optimum circuit parameters.

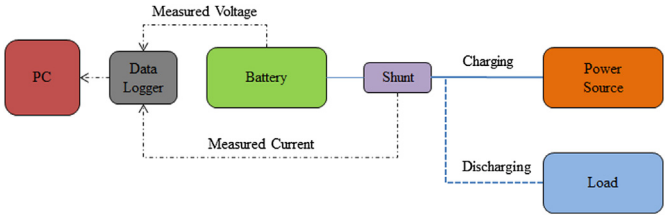

Fig. 7. The block diagram of the battery test apparatus.

The main advantage of the proposed algorithm over other parameter estimation algorithms is that during the parameter estimation process the time constants of the RC networks are kept constant, because they are the preferred approximation that fits the bandwidth of the battery application.

5. Experimental results on 14.4 V, 6.8 Ah lithium-ion battery modules

In this section, four Ultralife UBBL10 lithium-ion battery modules of the same age were used for tests, as numbered #1, #2, #3, and #4. These four batteries were in the same condition after having been left on the shelf for 2.5 years with good maintenance. The battery model was built on #1 based on behavior tests, and then the completed model was verified on #1, #2, #3, and #4 with the same performance tests. All the tests were conducted at room temperature. Results verified that the battery model built on battery module #1 was accurate when tested with the performance test, and it was robust enough to be used to represent other battery modules of the same kind. It was also shown that the module-to-module variation is less than the cell-to-cell variation, presumably a result of cell averaging.

5.1. Test apparatus

A block diagram of the battery test apparatus is shown in Fig. 7 and an image of the physical system is given in Fig. 8. The power source is a Sorensen SGI 60-V/500-A programmable power supply. The load is a Sorensen M540071-01 SLM 60-V/60-A 300-W DC Electronic Load. The shunt is a 5-mΩ resistor rated for 10 A. The current is calculated from the shunt voltage divided by the shunt resistance; the battery voltage is measured from the battery terminals. The data logger is an Agilent 34970A Data Acquisition/Data Switch Unit.

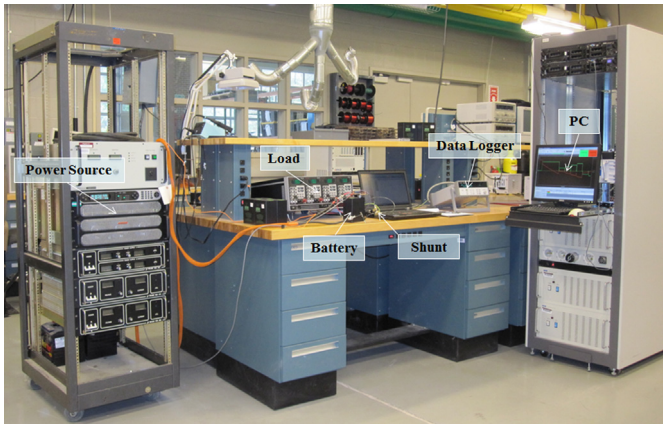

Fig. 8. Battery test apparatus.

Fig. 9. The 6.8 Ah Ultralife UBBL10 lithium-ion battery module.

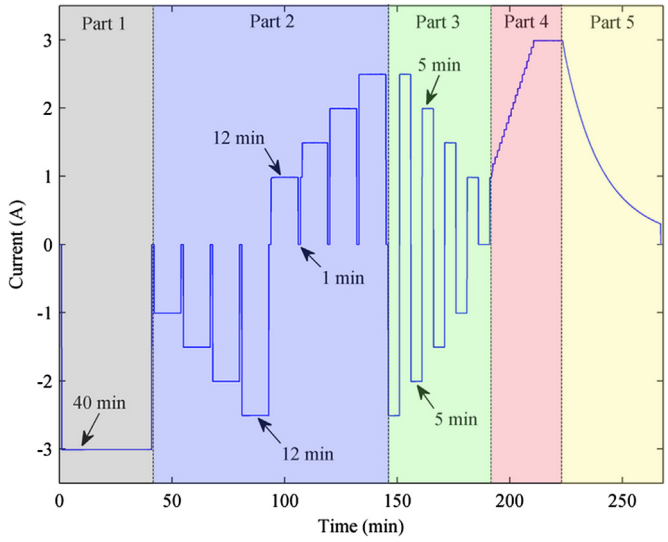

Fig. 10. The behavior battery test profile conducted on battery #1.

5.2. The Ultralife UBBL10 lithium-ion battery modules

The proposed approach was experimentally verified on a 6.8 Ah Ultralife UBBL10 lithium-ion battery module as shown in Fig. 9. It has two sections, which can be configured in series or parallel. In this test one section is used with a nominal voltage of 14.4 V [28]. The voltage range for each section is 10 V–16.5 V. In each section, there are three battery cells in parallel and four cells in series. Altogether in each section there are 12 cells. The battery cell is a Panasonic CGR18650 with a nominal voltage of 3.6 V and a standard capacity of 2450 mAh [31]. The cathode is made with lithium cobalt oxide; the anode is made with carbon [32]. A smart circuit is included in the battery module for cell-equilibration and protection. The battery module came with a display on top of the battery module with four levels of SOC indication.

Table 1
Estimated circuit parameters for the Ultralife battery module.

R_S (Ω)	R_1 (Ω)	C_1 (kF)	R_2 (Ω)	C_2 (kF)
0.1472	0.0338	1.7778	0.0446	47.1010

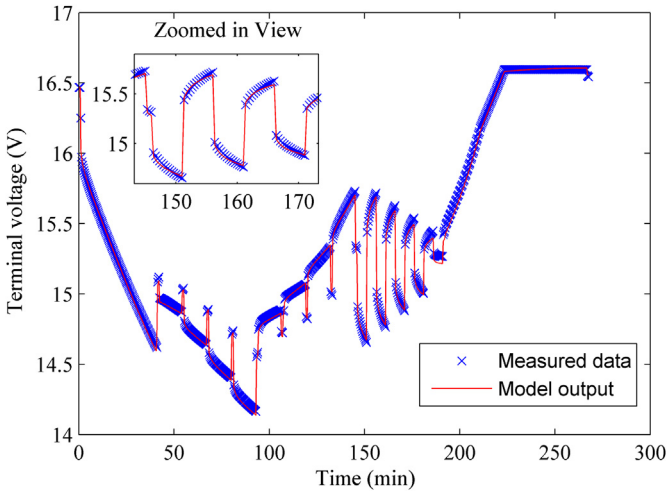

Fig. 11. Terminal voltage estimation results with the estimated parameters.

5.3. Parameter extraction

Battery module #1 among the four modules was used for parameter extraction.

5.3.1. Model bandwidth and number of RC networks

Since two RC networks represent the current level of complexity commonly used in comparable work, two RC networks are used here. For illustration purposes, the time constants are predetermined as $\tau_1 = 60$ s and $\tau_2 = 2100$ s, which are assumed to have been determined to accommodate the bandwidth of a notional battery application. In practice, a spectral analysis of the battery application might be used to arrive at the time constant selection. An example of this approach is covered in Section 6 for the case of a 21 kWh lithium-ion battery used in a PHEV.

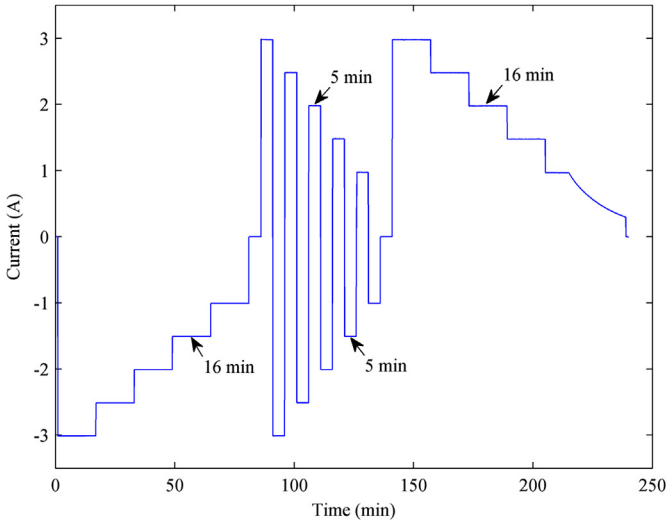

Fig. 12. The designed performance battery test profile for battery #1, #2, #3 and #4.

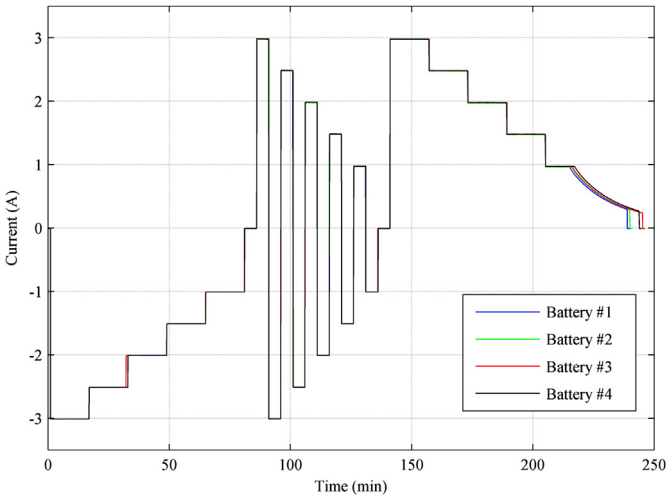

Fig. 13. The performance test current on battery #1, #2, #3 and #4.

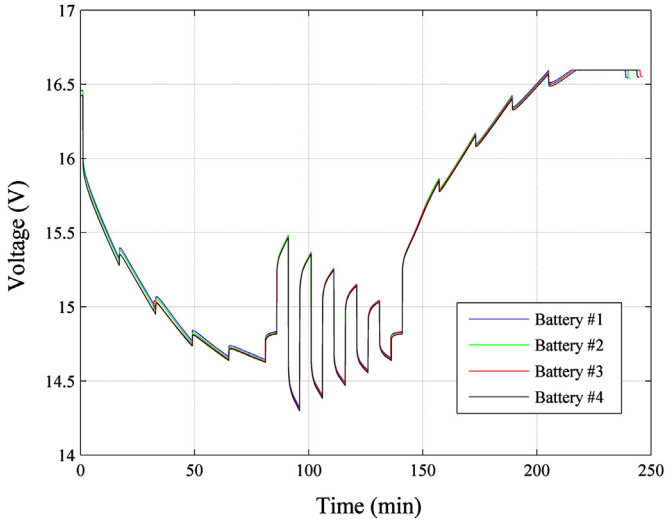

Fig. 14. The performance test voltage response on battery #1, #2, #3 and #4.

5.3.2. SOC–OCV profile extraction

The battery SOC–OCV profile was extracted from a battery experimental test as discussed in Section 4.3. The result is an 8th order polynomial equation correlating battery SOC and OCV.

5.3.3. Circuit parameter estimation

A behavior battery test was conducted on battery #1 for circuit parameter identification, as shown in Fig. 10. As the name "behavior" indicates, the battery test was designed to sufficiently excite the battery with different working conditions, which includes five parts. In the first part, the battery was discharged from full SOC to 70% SOC with 3 A constant current for 40 min. This allows the pulse charging/discharging tests to range between 50%

Table 2
Model verification results of the four battery modules.

UBBL10 battery #	1	2	3	4
MSE (1E-4 V^2)	5.04	6.748	4.464	5.243
Mean error (mV)	−8.269	−12.15	−5.131	−5.075
Max error (mV)	63.9	60	53.7	52.4
Rated error (%)	0.44	0.42	0.37	0.36

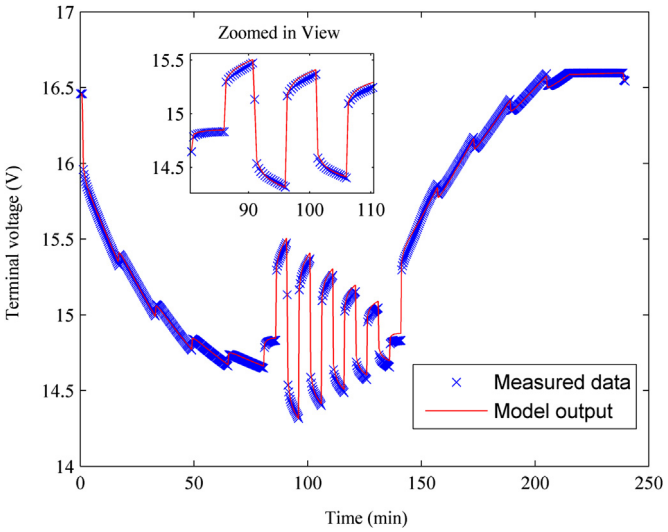

Fig. 15. Terminal voltage estimation results on battery #1.

Fig. 16. The A123 lithium-ion battery pack installed in the Mississippi State University EcoCAR.

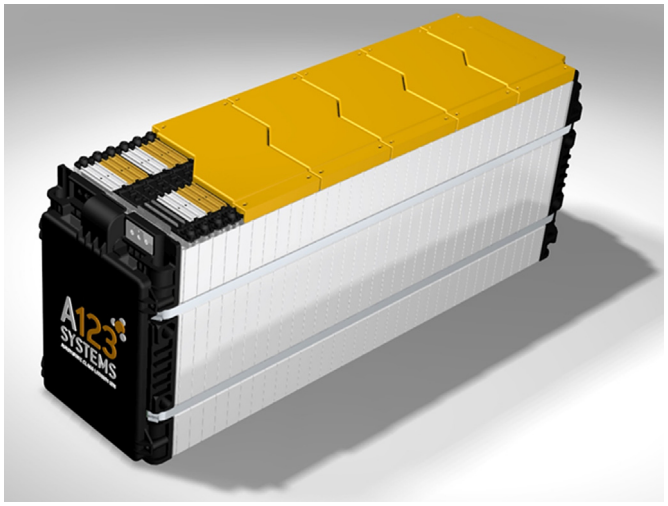

Fig. 17. The A123 battery module.

Fig. 18. The A123 prismatic battery cells.

and 70% SOC, which represents the desired battery normal operating range. This desired SOC operating range should be accommodated according to each specific application. In the second part, the battery was pulse discharged and charged with 1 A, 1.5 A, 2 A and 2.5 A currents. The length of the pulse was 12 min and the rest period was 1 min. The length of the pulse should be chosen based on the bandwidth of the application. Rest periods of 1 min were used to characterize the battery natural behavior while there was no external current excitation. In this part, the battery was discharged from 70% to 50% SOC and then charged back to 70% SOC. In the third part, the pulse discharging and charging currents were interleaved with 5 min pulse lengths without rest period. The currents used were 1 A, 1.5 A, 2 A and 2.5 A. This part represents faster dynamics than the dynamics in part 2. The pulse length should also be altered to accommodate the actual battery application bandwidth. In the fourth part, gradually increasing current from 1 A to 3 A followed by a constant 3 A current were used to charge the battery until the terminal voltage reached the voltage limit of 16.6 V, as defined in the datasheet. This step represents a different battery usage condition than part 2 & 3. After the battery terminal voltage reaches this voltage, the battery charging went to voltage controlled mode. In the fifth part, the battery was charged with controlled voltage of 16.6 V, until the current tapers to 300 mA, which defines 100% SOC in the datasheet. This represents a voltage float mode of the notional battery application.

Using the proposed parameter estimation algorithm, the parameters were estimated as shown in Table 1. The sheer size of the capacitor values illustrates the behavioral, rather than physics based nature of the model. With the estimated parameters, the model output voltage was compared with the measured battery terminal voltage, as shown in Fig. 11. Although the battery terminal voltage estimation looks accurate, this comparison will not be taken as model verification, as the measured terminal voltage was used to curve fit during the parameter estimation process. An independent performance battery test is used for model verification.

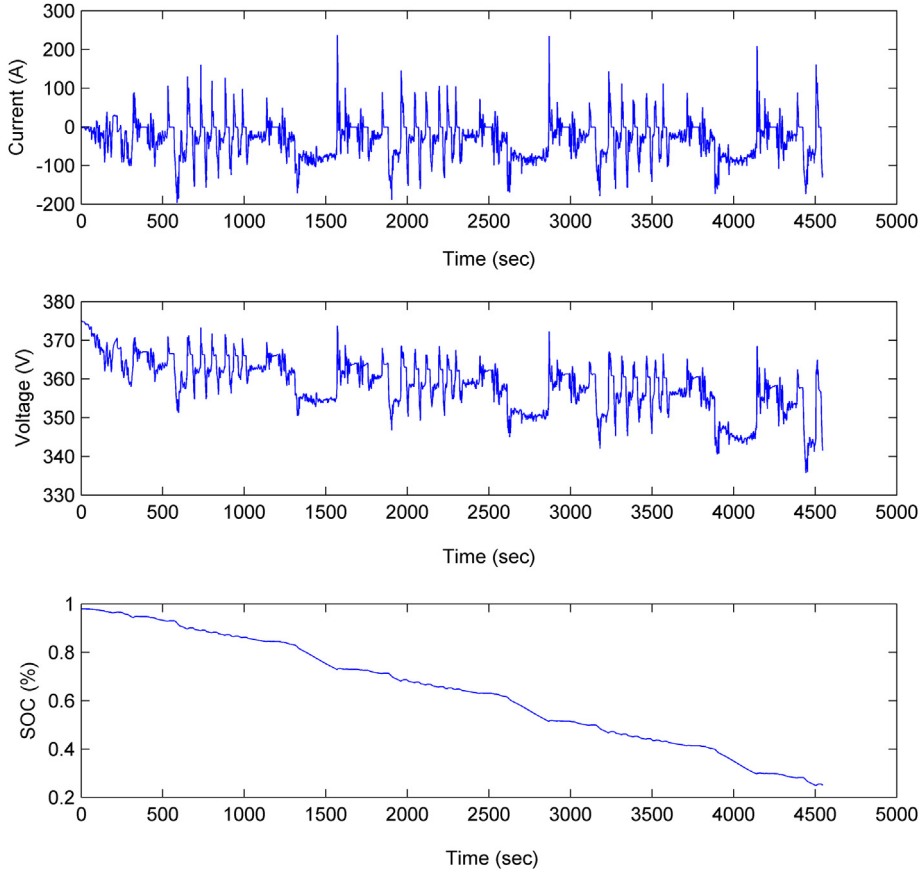

Fig. 19. The battery terminal current, terminal voltage and battery SOC during the on-vehicle battery test (behavior test).

As common criteria for battery model accuracy is the rated error, which is calculated as the max error between the measured and modeled battery voltage divided by the battery nominal voltage. The rated error is 0.41% in this case.

5.4. Model verification

To verify the robustness of the battery model with parameters estimated using battery #1, a different test profile was designed as shown in Fig. 12 and imposed on other battery modules from the same batch. The performance test current includes five current rates: 1 A, 1.5 A, 2 A, 2.5 A and 3 A, with pulse lengths of 5 min and 16 min. This performance test current has similar bandwidth with the behavior test current, which is the key to conserve the accuracy from the behavior test to the performance test. As illustrated in Section 4, in a real application the performance test profile, which usually is the actual working environment for the battery, is determined first, and then a behavior battery test is designed to sufficiently excite the battery with a bandwidth similar to the working environment. The current in Fig. 12 is actually the measured current from battery #1 during the performance test. Fig. 13 includes all the test currents on battery #1, #2, #3 and #4. In most parts, the current from the four batteries overlapped each other. Although it was intended to control the test stimulus to have exactly the same current, there were minor differences in the current because of the manual nature of the experimental test set up. The current variations at the end of the performance test, while charging the batteries to the full state of charge, reflect the battery module variations. Fig. 14 shows the measured battery terminal voltage during the battery performance test with a max voltage difference of 0.17 V (1.2% rated) among the four battery modules.

The statistical errors from open loop battery terminal voltage estimation with the electrical analogue battery model with the parameters estimated using battery #1 are shown in Table 2. The rated error on battery #1 is 0.44%, while the rated errors on battery #2, #3 and #4 are 0.42%, 0.37% and 0.36%, respectively. The statistical errors indicate that the model accuracy (0.41% error from behavior test) was conserved when the battery model was used with a different test profile, or even on other batteries from the same batch. As an example of the open loop battery terminal voltage estimation results, Fig. 15 shows the results from battery #1. The terminal voltage estimation results from battery #2, #3, and #4 are not plotted here, because they are so similar to Fig. 15.

5.5. Discussion

From the model verification, we can conclude that the proposed battery modeling approach can be successfully applied to module-level batteries. The completed electrical analogue battery model proved to be accurate (less than 0.44% error) and robust when tested against four battery modules of the same kind in similar performance battery tests.

6. Experimental results on a 360 V 21.3 kWh lithium-ion battery pack

In this section, the proposed battery modeling approach was applied to a large battery pack—an A123 360 V, 21.3 kWh lithium-ion battery pack, which was installed on the Mississippi State University EcoCAR (PHEV) [33]. A complete modeling of the A123 battery pack, illustrating the modeling process, is explained in this section as an example of a real-world application of the proposed battery modeling approach. Three sets of battery data were acquired for the modeling purpose. One set of data came from a pulse discharging–charging cycle on the battery pack (off-vehicle) for the purpose of battery pack SOC–OCV profile extraction. The other two sets of data were collected in the vehicle on a chassis dynamometer. One of them was used as behavior test data for model circuit parameter estimation; the other one was used as performance test data for battery pack model verification. The A123 "behavior" and "performance" data came from custom drive cycles for plug-in hybrid electric vehicle evaluation used by the EcoCAR competition program.

6.1. The A123 lithium-ion battery pack

The A123 lithium-ion battery pack representing the cutting-edge lithium-ion battery technology is shown in Fig. 16, where the battery pack is installed in the Mississippi State University EcoCAR. This battery pack includes five A123 battery modules (Fig. 17) connected in series. In each battery module, there are 22 prismatic battery cells (Fig. 18) in series and three in parallel. So altogether there are 66 battery cells in each battery module. Each battery cell has a capacity of 20 Ah and a nominal voltage of 3.2 V. A

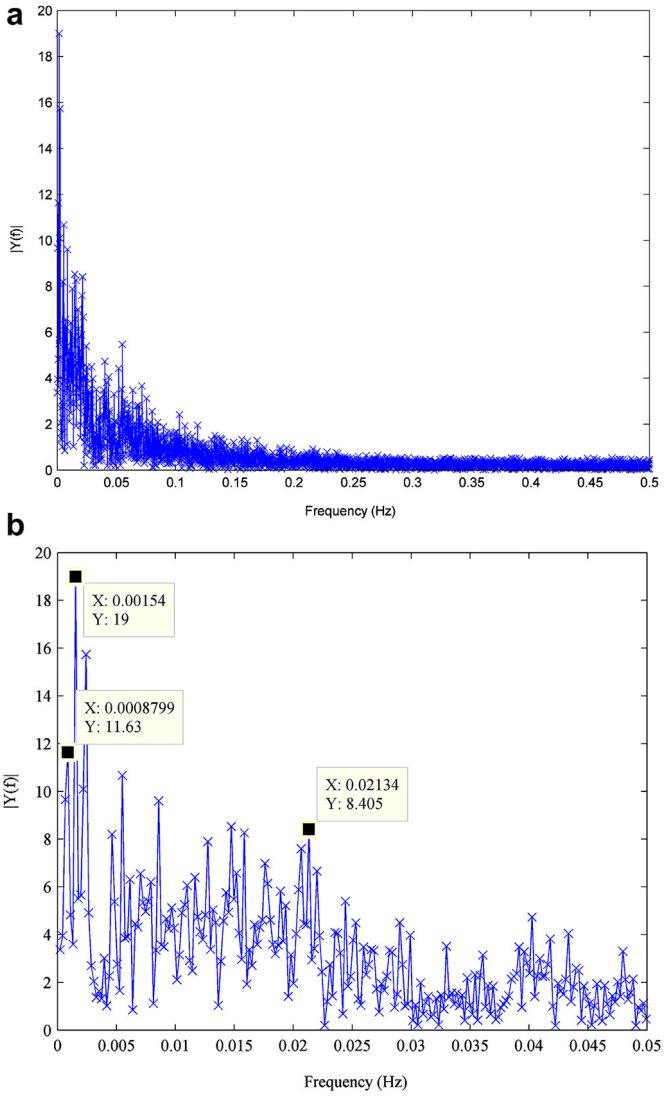

Fig. 20. The single-sided amplitude spectrum of battery terminal current (a) overview (b) close look.

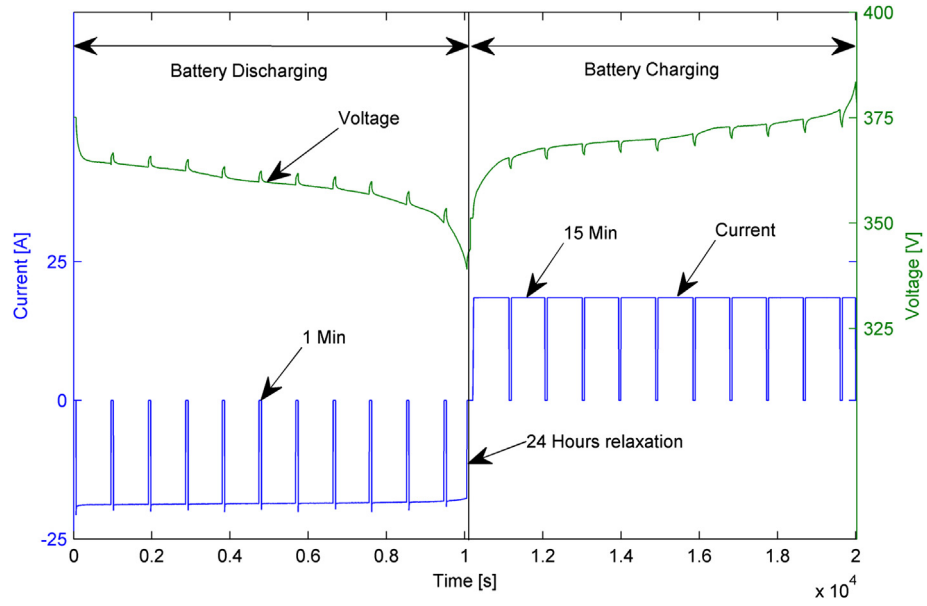

Fig. 21. The off-vehicle battery pack test for SOC–OCV extraction.

well-designed battery control module is included in the battery module to ensure safe operation of the battery pack. The detailed configuration of the battery module is provided here for reference only. The proposed modeling approach focuses on the battery external characteristics at the system level and neither requires nor uses such internal detail.

6.2. Parameter extraction

6.2.1. Model bandwidth and number of RC networks

With the data of the battery pack acquired from vehicle drive cycle testing while the battery pack was operated on-vehicle, it is possible to analyze the frequency of the battery application by doing a Fourier analysis of the battery terminal current. The battery terminal current, terminal voltage and battery SOC during the on-vehicle battery test were shown in Fig. 19. A single-sided amplitude spectrum of battery terminal current is shown in Fig. 20(a) and (b). From the spectral analysis of the battery current stimulus, the major frequency components range from 0.0008799 Hz to 0.02134 Hz.

With the major frequencies of the battery application identified, the bandwidth of the battery model should be in the same range. Thus the range for the time constants of the RC networks should be chosen as [1/0.02134 s, 1/0.0008799 s], which is [47 s, 1137 s].

The number of RC networks is chosen as two; however, this number should increase as the model fidelity requirement increase. In this case, the time constants of the RC networks in the battery model are determined as: $\tau_1 = 47s$ and $\tau_2 = 1137s$. For example, if a more accurate battery pack model is desired with three RC

Table 3
Estimated circuit parameters for the A123 battery pack.

R_s (Ω)	R_1 (Ω)	C_1 (kF)	R_2 (Ω)	C_2 (kF)
0.0764	0.0776	0.6053	0.0779	14.5982

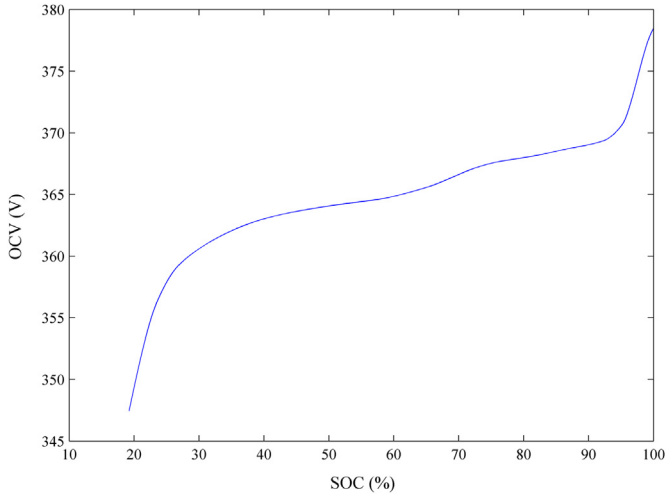

Fig. 22. The extracted SOC–OCV profile for the A123 battery pack.

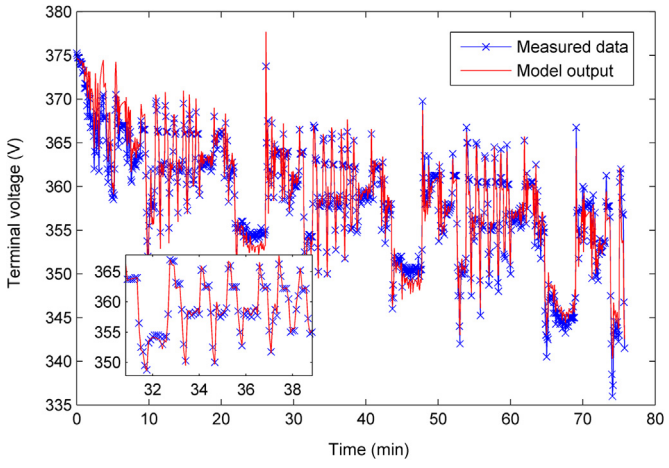

Fig. 23. The battery pack terminal voltage estimation results with the estimated parameters (behavior test).

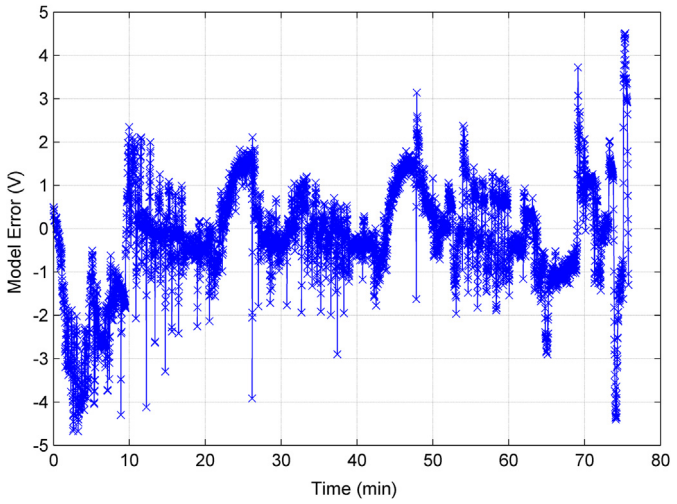

Fig. 24. The battery pack terminal voltage estimation errors (behavior test).

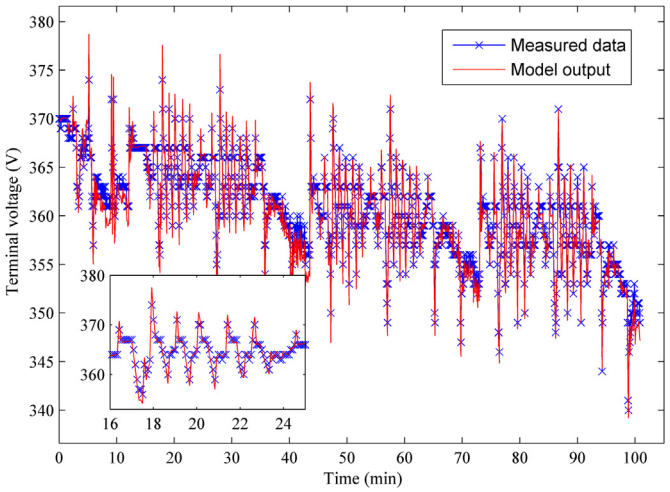

Fig. 26. The battery pack terminal voltage estimation results (performance test).

networks, the third time constant could be chosen as $\tau_3 = 1/0.00154s = 649.4s$, which is located between τ_1 and τ_2.

6.2.2. SOC–OCV profile extraction

To extract the SOC–OCV profile, an off-vehicle battery pack test was performed in the laboratory as shown in Fig. 21. In this test, the battery pack was discharged from full SOC with pulse discharging, left to rest for 24 h, and then charged back to full SOC with pulse charging. The discharging and charging pulse length was chosen as 15 min, which in each interval charged or discharged the battery pack by about 10% SOC. At the end of each charging/discharging pulse, the battery was allowed to rest for 1 min for relaxation. With the SOC–OCV profile extraction method described in Section 4.3, the extracted profile was shown in Fig. 22.

6.2.3. Circuit parameter estimation

The on-vehicle battery pack test data used for bandwidth analysis was used for circuit parameter estimation. During this step, the time constants of the circuit parameters are predetermined as [47 s, 1137 s]. The estimated parameters are shown in Table 3. Fig. 23 shows the battery pack terminal voltage estimation results with the estimated parameters, with the errors shown in Fig. 24. The mean error for the terminal voltage estimation is 0.52 V.

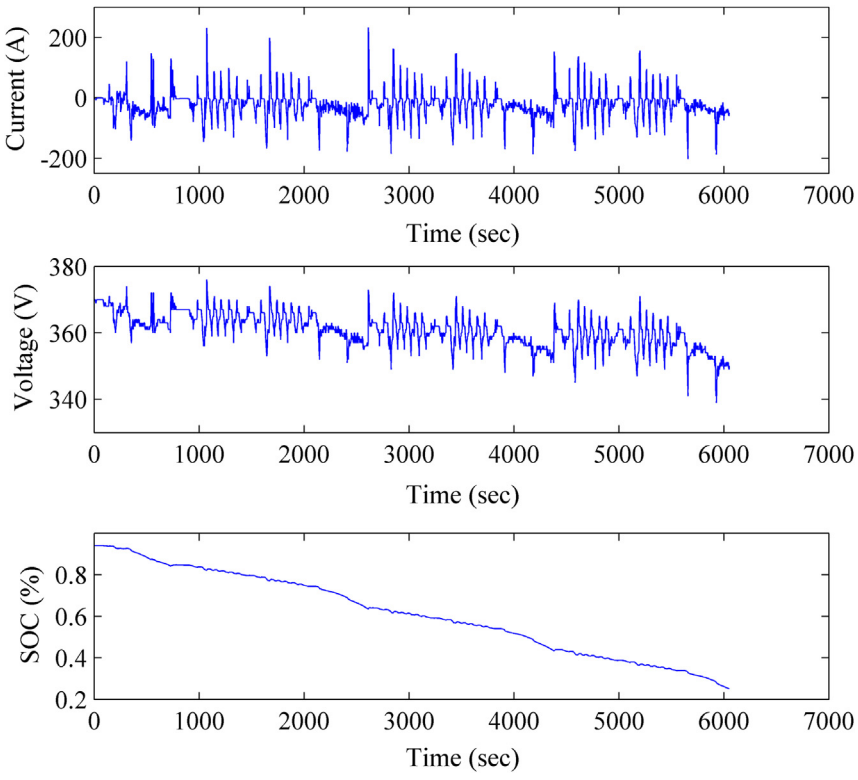

Fig. 25. The battery terminal current, terminal voltage and battery SOC during the on-vehicle battery test (performance test).

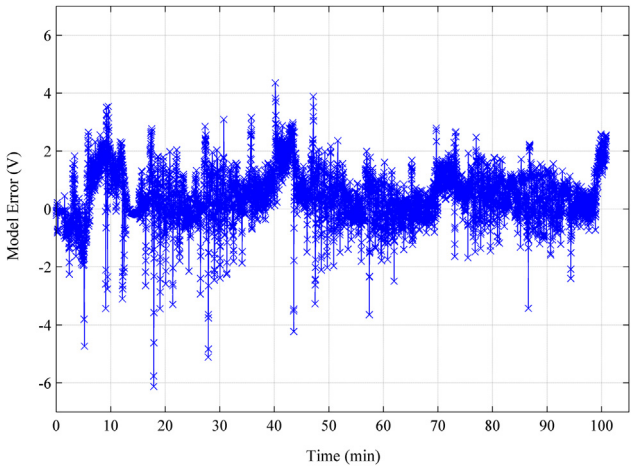

Fig. 27. The battery pack terminal voltage estimation errors (performance test).

Table 4
Estimated circuit parameters with arbitrary model bandwidth for comparison.

R_s (Ω)	R_1 (Ω)	C_1 (kF)	R_2 (Ω)	C_2 (kF)
0.0223	0.0029	68.9508	0.1203	16.6238

6.3. Model verification

The completed battery pack model with the extracted SOC–OCV profile and circuit parameters was verified with a different on-vehicle test profile as shown in Fig. 25. A spectral analysis of this test current stimulus shows that the new test current has similar bandwidth of [0.0004957 Hz, 0.01702 Hz] with the battery model ([0.0008799 Hz, 0.02134 Hz]). With the measured battery pack terminal current as the input to the battery pack model, the battery terminal voltage estimation results were plotted in Fig. 26, with the errors shown in Fig. 27. For the estimation results, the mean terminal voltage estimation error is 0.4112 V. 99.87% of the calculated errors were bounded within ±4 V, which is remarkably accurate considering the battery nominal voltage of 360 V. The rated error can be calculated as 1.11% of the nominal battery pack voltage, although this particular model did not include the benefit of the SOC–OCV profile correction procedure; if it had, it can be expected that less than 1% error would have been observed.

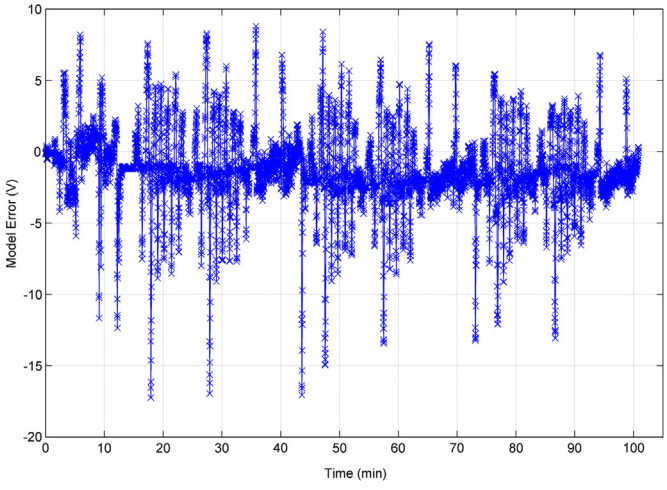

Fig. 28. The battery pack terminal voltage estimation errors (performance test) with an arbitrary selection of model bandwidth for comparison.

Table 5
Model accuracy comparison with different model bandwidth.

Bandwidth selection method	Time constants (s)	Mean error (V)	MSE (V^2)	Rated error
Proposed spectral analysis	[47, 1137]	0.4112	0.9649	1.11%
Arbitrary selection	[0.2, 2]	1.274	8.786	4.17%

6.4. Results comparison with an arbitrary selected model bandwidth

For comparison, an arbitrary selected model bandwidth was used with the same parameter estimation method and test data. The selected bandwidth is [0.5 Hz, 5 Hz], where $\tau_1 = 0.2\,s$ and $\tau_2 = 2\,s$ (compared with $\tau_1 = 47\,s$ and $\tau_2 = 1137\,s$). The estimated circuit parameters are shown in Table 4.

With the same model verification procedure detailed in Section 6.3, the estimation errors are shown in Fig. 28. Much increased terminal voltage estimation errors are observed from this figure. The mean terminal voltage estimation error is 1.274 V (compared with 0.4112 V). Since 99.83% of the calculated error could be bounded within ±15 V, the rated error can be calculated as 4.17% (compare with 1.11%) of the nominal battery pack voltage. The comparison results are summarized in Table 5.

6.5. Discussion

The use of the direct battery pack modeling approach towards a Lithium-ion battery pack used in an actual PHEV systematically illustrates the way the proposed approach can be used in real-world automotive applications. We can conclude that the proposed battery modeling approach is clearly suitable for battery packs, while maintaining the model accuracy (less than 1.11% error for a 360 V battery pack). We also observed that constant model parameters (not current dependent or SOC dependent) could be used in the electrical analog battery model without compromising the high fidelity even with aggressive current cycling up to 237 A. Although some researchers argue that the parameters should be current dependent or SOC dependent [4,5,12,15], it is shown here that satisfactory results can be achieved with constant parameters; a feature that has significant practical benefits over physical representations.

7. Conclusions

A direct battery pack modeling approach aimed at automotive applications is reported in this paper. A simple electrical analogue battery model is used for the battery pack behavioral representation with high accuracy. The focus of the reported work is the modeling of the external characteristics of the battery pack, and thus detailed materials and interconnection information about the battery pack are not required. A new level of fast dynamic battery pack simulation with high fidelity is enabled by embedding the bandwidth of the battery application into the bandwidth of the battery pack model. The reported approach was firstly verified on four Ultralife UBBL10 14.4 V, 6.8 Ah lithium-ion battery modules, with less than 0.44% modeling error and with good robustness over similar battery modules. And then this approach was used to model an A123 360 V, 21.3 kWh lithium-ion battery pack installed on a PHEV, with less than 1.11% modeling error shown during vehicle drive cycle tests. Since electrical circuit components are used in the

battery pack model, it is ideal for use in Matlab/Simulink and circuit simulation software. The reported battery pack modeling approach is independent of battery chemistries, thus applicable to lithium-ion, NiMH, and lead-acid batteries, among others. Temperature and lifetime effects, while not addressed in this work, can be included without changing the form of the model. These are two important practical issues that should be investigated in future work.

Acknowledgment

The authors gratefully acknowledge Dr. Marshall Molen and Matt Doude for supplying the A123 battery data and pictures. The authors would also like to thank James Gafford and Chris Parker for assistance in Ultralife UBBL10 battery test set up and data collection.

References

[1] W. Zhang, D. Dong, I. Cvetkovic, F.C. Lee, D. Boroyevich, in: Energy Conversion Congress and Exposition (ECCE) 2011, pp. 3270–3277.
[2] Y. Chen, G. Li, F. Zhang, in: 2011 International Conference on Electric Information and Control Engineering (ICEICE) 2011, pp. 2601–2604.
[3] O. Tremblay, L.-A. Dessaint, A.-I. Dekkiche, in: Vehicle Power and Propulsion Conference, Ieee, 2007, pp. 284–289.
[4] M. Chen, G.A. Rincon-Mora, IEEE Transactions on Energy Conversion 21 (2006) 504–511.
[5] L. Gao, S. Liu, R.A. Dougal, IEEE Transactions on Components and Packaging Technologies 25 (2002) 495–505.
[6] B. Schweighofer, K.M. Raab, G. Brasseur, IEEE Transactions on Instrumentation and Measurement 52 (2003) 1087–1091.
[7] A.A.-h. Hussein, N. Kutkut, I. Batarseh, in: Applied Power Electronics Conference and Exposition (APEC) 2011, pp. 1790–1794.
[8] J. Zhang, S. Ci, H. Sharif, M. Alahmad, in: Applied Power Electronics Conference and Exposition (APEC) 2010, pp. 672–675.
[9] S. Abu-Sharkh, D. Doerffel, Journal of Power Sources 130 (2004) 266–274.
[10] A. Shafiei, A. Momeni, S.S. Williamson, in: Vehicle Power and Propulsion Conference (VPPC) 2011, pp. 1–5.
[11] C. Sen, S. Member, N.C. Kar, S. Member, in: Vehicle Power and Propulsion Conference (VPPC) 2009, pp. 207–212.
[12] R.C. Kroeze, P.T. Krein, in: Power Electronics Specialists Conference (2008), pp. 1336–1342.
[13] J. Kim, J. Shin, C. Chun, B.H. Cho, IEEE Transactions on Power Electronics 27 (2012) 411–424.
[14] M. Dubarry, N. Vuillaume, B. Liaw, Journal of Power Sources 186 (2009) 500–507.
[15] N. Watrin, D. Bouquain, B. Blunier, A. Miraoui, in: Vehicle Power and Propulsion Conference (VPPC) 2011, pp. 1–5.
[16] M. Zheng, B. Qi, X. Du, in: 4th IEEE Conference on Industrial Electronics and Applications (ICIEA) 2009, pp. 2867–2871.
[17] R. Carter, A. Cruden, P.J. Hall, A.S. Zaher, IEEE Transactions on Energy Conversion 27 (2012) 21–28.
[18] S. Lajeunesse, in: The Applied Power Electronics Conference and Exposition (Apec) 2012.
[19] J. Li, M. Mazzola, J. Gafford, B. Jia, M. Xin, Journal of Power Sources 218 (2012) 331–340.
[20] J. Li, M. Mazzola, J. Gafford, N. Younan, in: Applied Power Electronics Conference and Exposition (APEC) 2012, pp. 427–433.
[21] K.M. Tsang, L. Sun, W.L. Chan, Energy Conversion and Management 51 (2010) 2857–2862.
[22] C.Y. Wang, V. Srinivasan, Journal of Power Sources 110 (2002) 364–376.
[23] C.M. Shepherd, Journal of The Electrochemical Society 112 (1965) 252–257.
[24] A.A.-h. Hussein, I. Batarseh, in: Power and Energy Society General Meeting, 2011, pp. 1–6.
[25] G. Plett, Journal of Power Sources 134 (2004) 262–276.
[26] G. Plett, Journal of Power Sources 134 (2004) 252–261.
[27] G.L. Plett, Journal of Power Sources 134 (2004) 277–292.
[28] Ultralife, UBI-2590 SMBus Technical Datasheet (2009), pp. 1–3.
[29] J.S. Arora, Introduction to Optimum Design, McGraw-Hill, 1989.
[30] P.E. Gill, Practical Optimization, Academic Press, 1981.
[31] Panasonic, Panasonic CGR18650DA Datasheet (2007).
[32] Panasonic, http://panasonic.com/industrial/includes/pdf/Panasonic_LiIon_Overview.pdf, 2007.
[33] M. Doude, G.M. Molen, W. Brown, J. Hoop, J. Moore, W. Dickerson, in: SAE 2012 International Powertrains, Fuels & Lubricants Meeting, Malmo, Sweden, to be published.